

PAIR-Diffusion: Object-Level Image Editing with Structure-and-Appearance Paired Diffusion Models

Vidit Goel^{1*}, Elia Peruzzo^{1,2*}, Yifan Jiang³, DeJia Xu³, Nicu Sebe²,
Trevor Darrell⁴, Zhangyang Wang^{1,3}, Humphrey Shi^{1,5,6}

¹Picsart AI Research (PAIR), ²UTrento, ³UT Austin, ⁴UC Berkeley, ⁵UOregon, ⁶UIUC

<https://github.com/Picsart-AI-Research/PAIR-Diffusion>

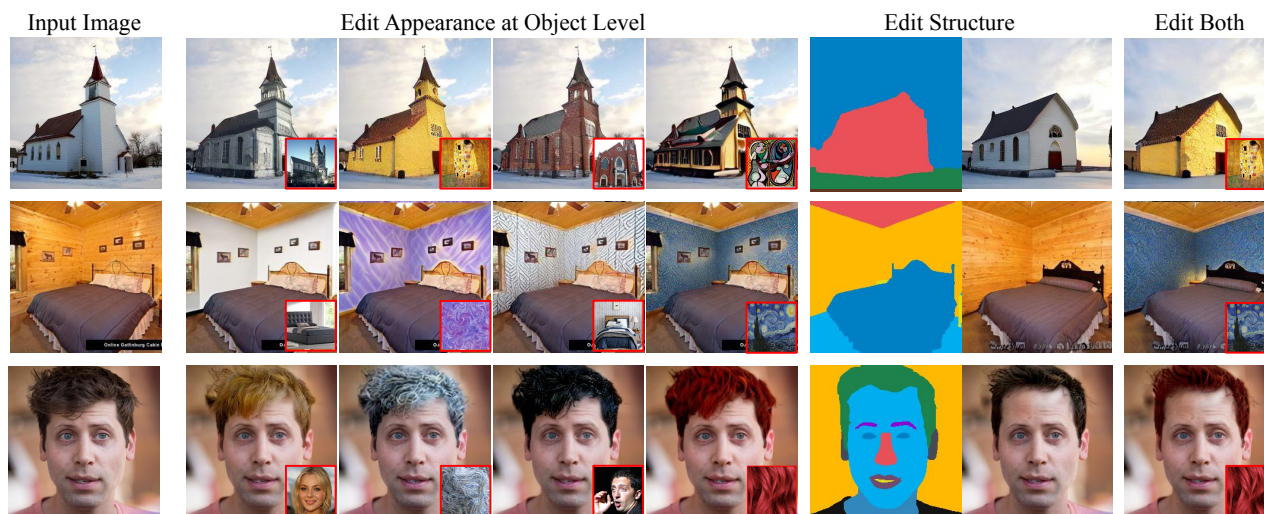


Figure 1: Structure-and-Appearance Paired (PAIR) Diffusion allows reference image-guided appearance manipulation and structure editing of an image at each single **object level**. These operations can either be performed independently or combined to provide users with comprehensive editing capabilities. All the displayed images are unseen during the training.

Abstract

Image editing using diffusion models has witnessed extremely fast-paced growth recently. There are various ways in which previous works enable controlling and editing images. Some works use high-level conditioning such as text, while others use low-level conditioning. Nevertheless, most of them lack fine-grained control over the properties of the different objects present in the image, i.e. object-level image editing. In this work, we consider an image as a composition of multiple objects, each defined by various properties. Out of these properties, we identify structure and appearance as the most intuitive to understand and useful for editing purposes. We propose Structure-and-Appearance Paired Diffusion model (PAIR-Diffusion), which is trained using structure and appearance information explicitly extracted from the images. The proposed model enables users to inject a reference image’s appearance into the input im-

age at both the object and global levels. Additionally, PAIR-Diffusion allows editing the structure while maintaining the style of individual components of the image unchanged. We extensively evaluate our method on LSUN datasets and the CelebA-HQ face dataset, and we demonstrate fine-grained control over both structure and appearance at the object level. We also applied the method to Stable Diffusion to edit any real image at the object level.

1. Introduction

Diffusion models have shown promising results for high-fidelity image generation and manipulation. With the introduction of large-scale text-to-image generative models, there has been a plethora of work on image editing. Many focus on text-based image editing [4, 21], while some use external guidance along with text such as reference image or segmentation maps [36, 61, 63] helping them get better control over the layout of the image. Different from previous works, we aim to independently control the proper-

*Equal Contribution

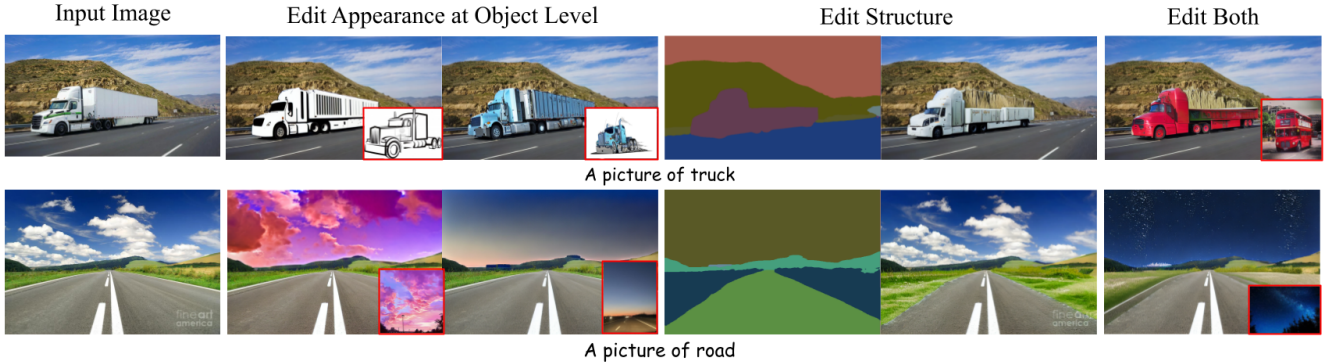


Figure 2: We explore appearance and structure control for images in the wild by applying our method to Stable Diffusion [50]. Our method enables unique editing capabilities, allowing image-guided appearance manipulation and structure editing at the object level for images in the wild. The text prompt is below each image. More details are provided in appendix E.

ties of multiple objects composing an image *i.e.* object-level editing. We refer to an object as both “things” and “stuff” [27, 45] composing the given image. Having independent fine-grained control over the properties of objects is an essential function if we want to edit images using diffusion models in an end-to-end manner. For example, given an image of a bedroom, the user should be able to precisely change the color or texture pattern of the bed by keeping the shape unaltered (or vice-versa), without affecting other objects (such as the ceiling or the wall) in the same image.

Existing image editing techniques can be categorized based on the level of control they have over individual objects in an image. One line of work involves the use of text prompts to manipulate images [4, 21]. However, these methods have limited capability for fine-grained control at the object level, owing to the difficulty of describing the shape and appearance of multiple objects simultaneously with text. In the meantime, prompt engineering makes the manipulation task tedious and time-consuming. Another line of work improves user control by leveraging the latent space of diffusion models [33, 66]. Nevertheless, they suffer from multi-object editing issues due to the disorganized and uninterpretable latent representations. Several other works [26, 36, 61, 63, 74, 76] explore the explicit method to manipulate objects’ shape, including segmentation maps [15, 74], binary masks [26], sketches [63], or bounding boxes [70]. However, most of these works either fall into the prompt engineering pitfall or fail to independently manipulate multiple objects.

To tackle the aforementioned issues, we propose a novel framework, dubbed Structure-and-Appearance **Paired Diffusion Models (PAIR-Diffusion)**. Specifically, we perceive an image as an amalgamation of diverse objects, each described by various factors such as shape, category, texture, illumination, and depth. Then we further identified two crucial macro properties of an object: structure and appear-

ance. Structure oversees high-level aspects such as an object’s shape and category, while appearance contains low-level details like texture, color, and illumination. To accomplish this goal, PAIR-Diffusion adopts an off-the-shelf network to estimate semantic segmentation maps as the structure, and then extract appearance representation by a pre-trained image encoder. We use the extracted per-object appearance and structure information to condition a diffusion model and train it to generate images.

In contrast to previous text-guided image editing works [3, 4, 9, 52], we consider an additional reference image to control the appearance. Compared to text prompts which only vaguely describe the appearance, images can precisely define the expected texture and make fine-grained image editing easier. Different from existing work [79] which focuses on applying in-domain examples as references, PAIR-Diffusion injects the appearance from an arbitrary reference image, either it is similar to the input sample or taken from in-the-wild scenes. Meanwhile, users can modify the structure of the scene while keeping the appearance of the individual objects unchanged. We present the editing capabilities of our method in Fig. 1. We also investigate the application of our method to foundation text-to-image diffusion models, and edit images in the wild with Stable Diffusion [50] in Fig. 2. Finally, we extend a new spatially-adaptive classifier-free guidance, which provides better control over structure and appearance components.

Our main contributions are summarized as follows:

- We propose PAIR-Diffusion, which allows the structure and appearance of each single object to be edited independently. It is trained using structure and appearance information explicitly extracted from the images.
- The proposed design can achieve various editing tasks using one unified model: injecting appearances from reference images either locally or globally, controlling

the strength of injection, and manipulating the layout while maintaining the overall appearance of objects.

- Additionally, we propose a new spatial classifier-free guidance, which helps in improving the editing capabilities of our proposed model.

2. Related Work

Diffusion Models. Diffusion probabilistic models [58, 23] function as advanced generative models that synthesize data through an iterative denoising process. These models employ a forward process, incorporating noise into data distributions and subsequently reversing the process to reconstruct the original data. Notably, Dhariwal *et al.* [12] introduced various techniques such as architectural improvements and classifier guidance, that helped diffusion models beat Generative Adversarial Networks (GANs [18]) in image generation tasks for the first time. Subsequently, numerous studies [39, 48, 50, 53] focused on scaling the models to billions of parameters, improving the inference speed [54] and memory cost [50, 62]. Especially, LDM [50] is a prominent model that decreases computational costs by applying the diffusion process to a low-resolution latent space, successfully scaling for text-to-image generation with web-scale data. Other than image generation, they have been utilized in various domains such as text-to-3D [44, 57], language generation [35], 3D reconstruction [20], novel-view synthesis [68], music generation [25, 37], etc.

Controllable Image Generation. Despite the tremendous success of image generation applications, the examples produced by deep generative models are generally disorganized. Several different works [32, 51, 8] try to mitigate this issue from texture/style and content/structure perspectives. Especially Xian *et al.* [67] apply texture patches as conditional factors, as well as the sketch input, to produce texture-dependent examples. Park *et al.* [40] propose a spatially-adaptive normalization layer (SPADE) that allows the generated images to be conditioned on an input segmentation map. Zhu *et al.* [79] further improves the performance of SPADE by introducing per-region style encoding. Different from others, BlobGAN [13] learns a mid-level representation in an unsupervised manner that controls the spatial position of each generated object. However, their results were limited to indoor scenes only. Analogously, there have been various works for controllable image generation using diffusion models [14, 15, 50, 64, 70, 75]. One line of prevalent approaches involves controlling images by the text prompts [38, 39, 49, 50], which is typically conveyed to diffusion models through cross-attention mechanisms. Later, Versatile Diffusion [69] further integrates text and images within a multi-flow, multi-modal framework designed for the simultaneous execution of multiple tasks. Nevertheless, text prompt offers only an approxi-

mate definition of an object’s position or appearance in images. To address this, several works employ spatial conditioning signals, such as images, segmentation maps, or sketches [14, 15, 64, 75]. The most advanced technique, ControlNet [76], presents an efficient, rapid method for augmenting existing text-to-image models with control elements, such as edges, segmentation maps, or depth maps. However, the appearance of their generated samples still heavily rely on the text prompts. Despite being intuitive, text may not be the optimal means to describe an object’s appearance under many scenarios. Instead, we propose to control the structure and appearance together, using reference images and spatial conditions.

Image Editing with Generative Priors. Deep generative models endeavor to create diverse and high-fidelity samples across multiple modalities. Starting from generative adversarial networks (GANs [19, 47, 30, 17, 29]), generative models show preliminary success by producing persuasive and compelling images with smooth latent space, thereby facilitating robust editing capabilities in subsequent tasks. Karras *et al.* [31] adopt a style space to improve GAN’s controllability by disentangling the style representation and content representation. Abdal *et al.* [1] propose to encode real-world samples into StyleGAN’s style space by iterative optimization which significantly increases the fidelity of reconstructed images, and helps further editing and manipulation tasks [2] accordingly. Another strand of research [43, 78] directly trains an encoder that can project real-world examples into the latent space of GAN without iterative optimization. Nevertheless, determining the appropriate editing direction remains challenging due to the style space being high-dimensional. This issue is mitigated by injecting language guidance into latent representations [42] with the assistance of CLIP encoders [46]. Analogously, several attempts [22, 38, 41] have been made on exploring the potential of diffusion models on editing tasks. InstructPix2Pix [4] enabled feed-forward image editing by adopting instruction-based data synthesis as the training pipeline. Pix2pix-zero [41] identifies an editing direction for a specific category and employs an attention mechanism to perform local editing in accordance with prompt guidance. Distinct from prior approaches, our methodology interprets images as compositions of various objects for editing purposes and suggests utilizing images, rather than text prompts, as a more precise and intuitive way to control the appearance of the objects.

3. Method

Given a sample of data points, the aim of the generative model is to learn the underlying distribution $p(x)$ from which the data was sampled. In the case of image generation, this is usually designed as a holistic process, where the chosen model learns to generate images as a whole in the

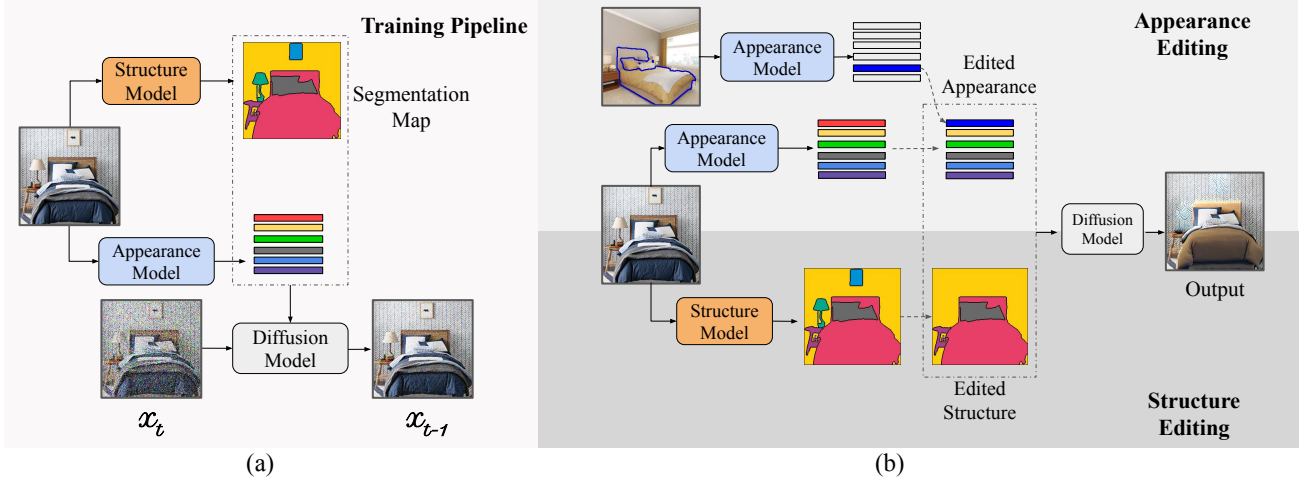


Figure 3: Overview of PAIR diffusion. An image can be seen as a composition of objects each defined by different properties like structure (shape and category), appearance, depth, etc. We focus on controlling structure and appearance. (a) During training, we extract structure and appearance information and train a diffusion model in a conditional manner. (b) At inference, we can perform multiple editing operations, independently controlling the structure and appearance of any real image at the object level.

pixel space [31, 50, 59]. Nevertheless, natural images can be seen as a composition of objects [65], each described by different factors, *e.g.* shape, style, texture, depth, illumination, etc. Under this formulation, $p(x)$ can be written as:

$$p(x) = \int p(x|z)p(z)dz \quad (1)$$

with $z = (o_1, o_2, \dots, o_N)$, N the number of objects, and o_i the latent variables associated with the i -th object describing different factors such as style, depth, or illumination.

In this work, we aim for fine-grained image editing. We thus assume that we already have the information about the objects that we want in the final image from references provided by the user. Therefore, we are only interested in the distribution $p(x|z) = p(x|(o_1, o_2, \dots, o_N))$. As discussed in Sec. 1, image editing should be interpretable and intuitive and we reflect this in the choice of the latent factors in o_i that we aim to explicitly control. In particular, we identify *shape*, *category*, and *appearance* as the most useful and intuitive for editing purposes and propose an efficient and convenient way to compute them. We then train a generative model conditioned on those factors to enable test-time real-image editing, showing multiple editing capabilities. In the following, we describe our method in detail: Sec. 3.1 discuss our choice of factors for object representation and how to train a model such that we can control them and edit real images, Sec. 3.2 gives a formal description of fine-grained image editing under our framework, while Sec. 3.3 describes the spatial classifier free guidance specifically introduced for editing purposes.

3.1. Structure and Appearance Paired Diffusion

We identify *shape*, *category*, and *appearance* as the most important factors a user wants to control. We define structure to contain both *shape* and *category*. We thus represent an object as $o_i = \{s_i, f_i, \pi_i\}$, where $s_i = \{c_i, m_i\}$ represents the structure, with category c_i and shape m_i , and f_i the appearance. π_i denotes a latent variable that captures all the aspects of the i -th object which we do not wish to control; we represent with $\pi = \{\pi_i\}$ the collection of these variables for all the objects in the image.

Our main intuition is that conditioning a generative model on mutually exclusive factors presents built-in capabilities for controlling the factors and editing images. Next, given a real image $x \in \mathbb{R}^{3 \times H \times W}$, we describe how object-level representations o_i can be extracted.

Structure. We represent the structure information using a segmentation map, due to the fine-grained control it provides and the ease of computation. Given an off the shelf network $E_S(\cdot)$, we obtain $S = E_S(x)$, with $S \in \mathbb{N}^{H \times W}$. Let c_i be the class of the i -th object as predicted by the segmentation network, we extract the shape as:

$$m_i[j, k] = \begin{cases} 1, & \text{if } S[j, k] = c_i \\ 0 & \end{cases} \quad (2)$$

with $m_i \in \{0, 1\}^{H \times W}$.

Appearance. The appearance information should majorly contain low-level information such as texture, color, and illumination. Hence, to extract appearance information, we use pre-trained encoder $E_F(\cdot)$ and select the features from early layers as they contain more low-level informa-

tion [16, 71, 73]. In practice, we compute $\tilde{F} = E_F(x)$, with $\tilde{F} \in \mathbb{R}^{C \times H' \times W'}$, where $H' \times W'$ is the resulting spatial size and C is the channel. We then parse object-level features, following Eq. (2) to pool over the spatial dimension:

$$f_i = \frac{\sum_{j,k} E_F(x) \odot m_i}{\sum_{j,k} m_i} \quad (3)$$

Model formulation. With the procedure described above, we have a deterministic way of obtaining $\{s_i, f_i\}$ from image x . Note that we do not expect to have control over other latent variables $\pi = \{\pi_i\}$, hence we can simply sample them from a known prior distribution. Given this formulation, we can rewrite Eq. (1) as:

$$p(x|S, F) = \int p(x|\{s_1, f_1\}, \dots, \{s_N, f_N\}, \pi) p(\pi) d\pi \quad (4)$$

where $S \in \mathbb{N}^{H \times W}$ is the output of the segmentation network, representing both *shape* and *category*, and $F \in \mathbb{R}^{N \times C}$ captures *appearance* information of the objects in the image. Finally, the task of fine-grained object-level image control boils down to learning $p(x|S, F)$, which can be formulated as a conditional generative model. In practice, we use the latent diffusion model (LDM) [50] to realize $p(x|S, F)$ because such models are efficient. Following nomenclature in the diffusion literature [23, 59], we refer to the learned model by $\epsilon_\theta(z_t, S, F)$, with z_t being the noisy latent variable. We condition the model by concatenating the segmentation map S , and the appearance features F which are spatially splatted in a tensor of shape $C \times H \times W$. We modify the model architecture to accommodate for the new input dimension, increasing the input channels of the first layer from C_{in} to $C_{in} + C + 1$. We keep the rest of the architecture unchanged and follow the training protocol described in [50]. We refer the reader to *Supp. Mat.* for additional details. At inference time, given (S, F) , we sample $z_T \sim \mathcal{N}(0, 1)$ and apply the DDIM algorithm [59] to obtain the final image. In the next section, we describe how this formulation can be used to edit images.

3.2. Object Level Image Editing

PAIR-Diffusion provides built-in control over structure and appearance, resulting in various editing capabilities. Given an input image x , the user can modify the structure of the objects and manipulate the appearance using a reference image as a driver. More importantly, the two functions are independent, giving full control to the end user. Let us assume the user wants to edit the i -th object, described by $o_i = \{s_i, f_i\}$. The structure of the object can be easily manipulated by modifying s_i , e.g. changing the shape of the object or completely removing it (see Fig. 3 (b), bottom).

Simultaneously, the user can change the appearance of the object using a reference image x^R . We use the appearance model to extract the reference appearance representation f^R and obtain the edited appearance as:

$$f_i^E = \alpha \cdot f_i + \beta \cdot f^R \quad (5)$$

with α, β controlling the strength of the manipulation (see Fig. 3 (b), top). Note that f^R can be extracted from a specific object of x^R , or using the whole reference image. Depending on the source of f^R , we distinguish two settings: *In Domain Appearance Manipulation* (ID) and *Out of Domain Appearance Manipulation* (OD). In ID, f^R should come from an object in the reference image that has the same category of o_i . We can do it by setting m_i appropriately in Eq. (3). In OD, f^R can be computed from any reference image which might not be semantically relevant to the underlying structure in the input image. This represents a much more challenging scenario and further proves the disentanglement between appearance and structure. Although we discussed editing with respect to one object, it is trivial to extend it to multiple objects.

After the user has performed the desired changes, we can sample the edited image using $\epsilon_\theta(z_t, S^E, F^E)$ where S^E, F^E denotes the edited structure and appearance representations. We notice that there are other object properties we do not explicitly control (denoted as π in Sec. 3.1). Therefore, randomly sampling different $z_T \sim \mathcal{N}(0, 1)$ will bring variety to our results while remaining consistent with the desired edits. When performing localized editing operations, we rely on masked DDIM sampling [50] to limit the changes to the desired region (see *Supp. Mat.*). To summarize, using PAIR-Diffusion, we can achieve the following editing capabilities (i) editing structure while keeping the appearance of the image similar, (ii) controlled appearance manipulation at the object level guided by a reference image both IN and OD. We provide extensive qualitative results for each case in Sec. 4. In the next subsection, we will discuss spatial classifier-free guidance, which improves independent control over structure and appearance.

3.3. Spatial Classifier-free Guidance

Classifier-free guidance [24] has been of great practical use in conditional diffusion models [50] to improve the sampling quality in terms of diversity. In practice, the diffusion model is trained jointly in a conditional and unconditional manner by dropping the conditions with some probability. Similarly, we also drop the structure or appearance conditioning with probability 0.1 during training. We never drop only the structure information, because appearance does not make sense without structure. At every time step t during inference time, the model is inferred in both a conditional and unconditional manner. Next, the output of the unconditional model is combined with the output of the conditional

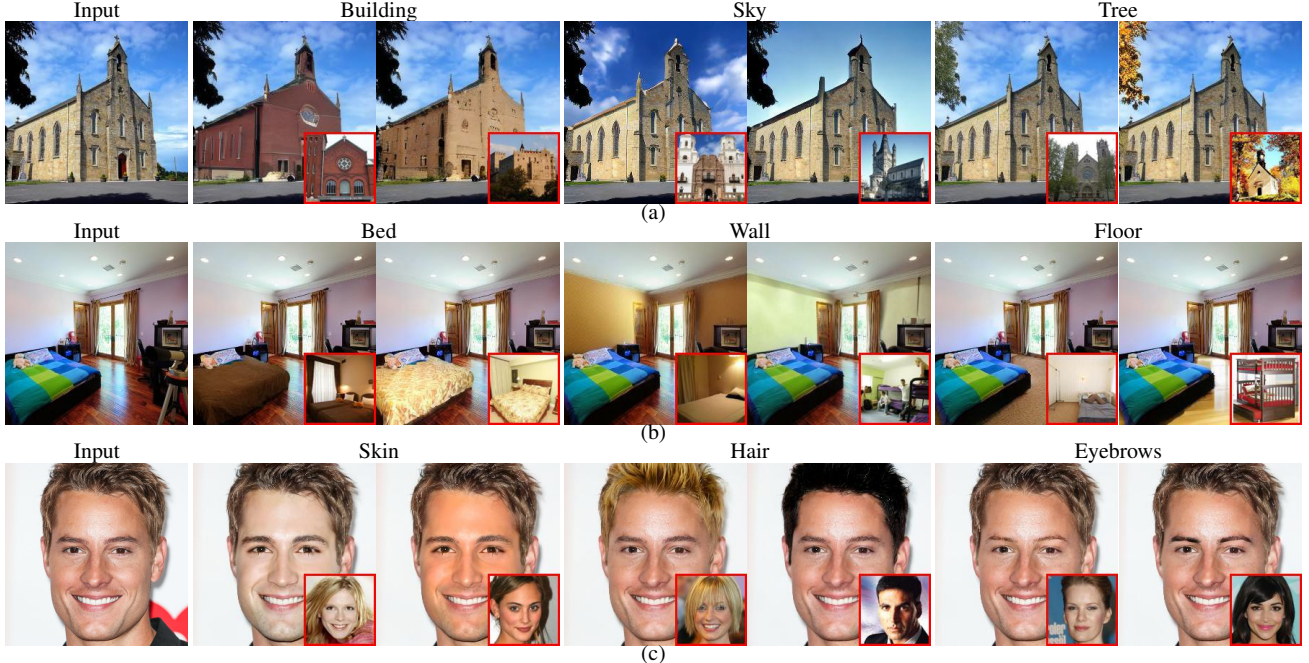


Figure 4: Qualitative results on In Domain Appearance Manipulation. Reference images are shown in the bottom right, while the text on top indicates the object targeted by the editing operation.

model. A straightforward application of this strategy would result in $\tilde{\epsilon}_\theta(z_t, S, F) = \epsilon_\theta(z_t, \phi, \phi) + s(\epsilon_\theta(z_t, S, F) - \epsilon_\theta(z_t, \phi, \phi))$, where s is a scaling factor. However, there can be cases when a particular appearance might not align well with the underlying structure. With the above formulation, structure and appearance are ruled by a single factor and we cannot give more importance to one over the other. Moreover, there can be multiple objects in the image and we would like to control them in an independent manner. For these reasons, we introduce two spatial scale factors $s_S, s_F \in \mathbb{R}^{H \times W}$ for structure and appearance respectively, and propose the *spatial classifier-free guidance*:

$$\begin{aligned} \tilde{\epsilon}_\theta(z_t, S, F) = & \epsilon_\theta(z_t, \emptyset, \emptyset) \\ & + s_S \cdot (\epsilon_\theta(z_t, S, \emptyset) - \epsilon_\theta(z_t, \emptyset, \emptyset)) \\ & + s_F \cdot (\epsilon_\theta(z_t, S, F) - \epsilon_\theta(z_t, S, \emptyset)) \end{aligned} \quad (6)$$

In this way, we can specify different strengths for the appearance and structure of different objects during inference.

4. Experiments

We extensively test our method both qualitatively and quantitatively. We train our models of several datasets of different sizes, respectively the bedroom and church partitions of the LSUN Dataset [72], and the CelebA-HQ Dataset [30]. Details about the training procedures can be found in *Supp. Mat.* Sec. 4.1 shows various editing capabilities that can be achieved with our method, Sec 4.2 compares

PAIR-Diffusion with other baselines in the task of localized image editing, while Sec 4.3 further discusses the role of structure and appearance as well as future directions.

4.1. Image Editing

In this section, we present the visual results of various editing operations. Note that all the editing visualizations are made using the images from the validation set of the respective dataset.

We start by showing the results for *In Domain Appearance Manipulation* in Fig. 4. Following the definition of Sec. 3.2, we swap the appearance of an object of the input image with the appearance of an object of the same class from the reference image (we set $\alpha=0, \beta=1$ in Eq. (5)). In Fig. 4 (a), we can notice that our method can easily transfer the appearance of a church from a completely different structure in the reference image to the structure of the church in the input image. At the same time, we can copy relatively homogeneous regions like the sky, transferring the color accurately, as well as more textured objects such as the trees. In Fig. 4 (b), it is interesting to note that, when we change the style of the floor, the model can appropriately place the reflections hence realistically harmonizing the edit with the rest of the scene. Similar observations can be made when we edit the wall. Lastly, in Fig. 4 (c) we show results on faces. We can observe that PAIR-Diffusion accurately transfers the appearance from the reference image, modifying the skin, hair, and eyebrows of the input. We notice that

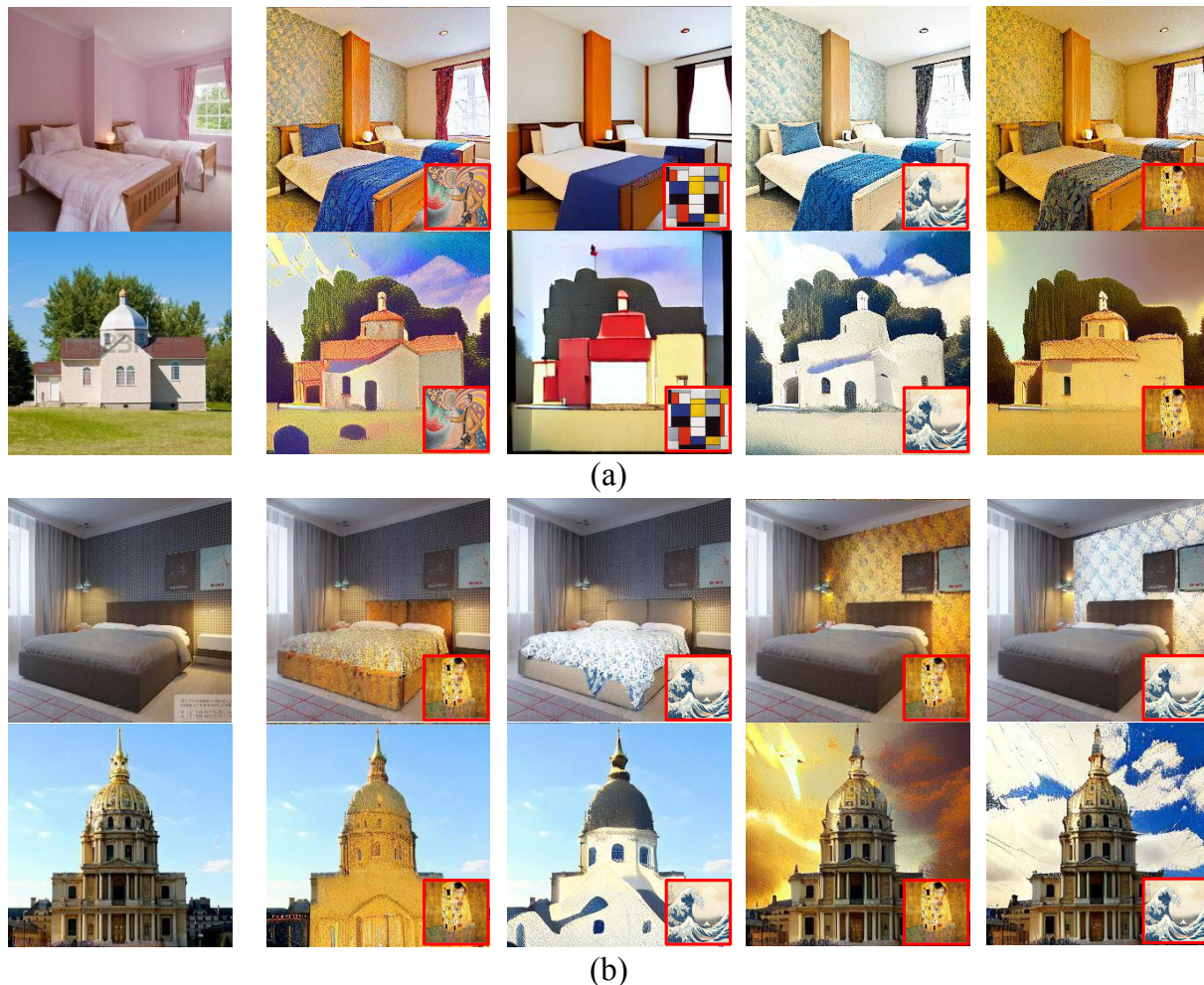


Figure 5: Qualitative results for Out of Domain Appearance Manipulation. The appearance of the reference image (bottom right) is transferred (a) globally, and (b) locally.

our edits never alter the identity of the person in the input image, which is desirable when editing faces.

Next, in Fig. 5, we investigate the potential of PAIR-Diffusion for *Out of Domain Appearance Manipulation*. As discussed in Sec. 3.2 this represents a more challenging scenario, as the appearance features computed from the reference image can be semantically irrelevant to the object we wish to edit, hence more difficult to render in a consistent manner. We compute a single appearance vector from the reference image, setting $m_i[j, k] = 1 \forall j, k$ in Eq.(2), and assign it to the object we want to edit, setting $\alpha = 0, \beta = 1$ in Eq.(5). In Fig. 5 (a), we analyze global manipulation where we change the appearance vectors of all the objects in the input image with the reference appearance vector, keeping only the structure unchanged. We can observe that PAIR-Diffusion seamlessly transfers both high-level concepts and color palettes from the reference image to the input image. For example, in the first column, the pointillism style of the

reference image is faithfully present in the edited result. At the same time when the reference image is composed of solid colors (second column), the same will be present in the edited image. Similar conclusions can be drawn from local manipulations shown in Fig. 5 (b). In this case, we transfer the appearance of the reference image to a localized area of the input image, keeping the structure and the appearance of the other objects unchanged. Analyzing the results of Fig. 5 (b), we can observe that the reference image is exploited in different ways, according to the semantics of the object we wish to edit in the input image. For instance, *the wave* image is transferred as a repetitive pattern when targeting the wall (fourth column, first row), while it conveys homogeneous colors when copied to the sky (fourth column, second row).

Lastly, we analyze the structure editing capabilities of PAIR-Diffusion in Fig. 6. With our method, we can effectively modify the shape of fine-grained objects (first row),

remove objects from the scene (second row), as well as more coarse structure modification (last row). Note that the appearance of the objects does not change when editing the structure component. We refer the reader to *Supp. Mat.* for additional qualitative results and editing applications, e.g. interpolation.

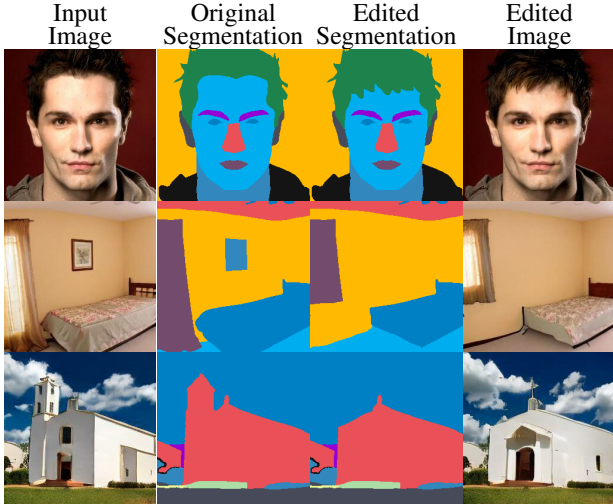


Figure 6: Qualitative results for structure manipulation of the input image. Our method can edit the structure, without changing the appearance of the objects.

4.2. Quantitative Experiments

We begin with evaluating the performances of our method for the task of *in domain appearance editing*. In this task, we edit a specific region of the input image, using as a reference a target image from the same class. We compare our method with the recent work of Brown *et al.* [5], and follow their evaluation procedure. In particular, different models are compared based on: (i) Naturalness: we expect the edited image to look realistic (we rely on FID between input and edited images to assess it), (ii) Locality: we expect the edit to be limited to the specific region where the edit is performed (we measure it with L1 loss), (iii) Faithfulness: we expect the edited region and the target image to be similar (we use SSIM to evaluate it). As discussed in [5], all the above-mentioned criteria should hold at the same time, and the best-performing method is the one giving good results in the three metrics at the same time. We compare our method with four baselines: (1) Copy-Paste: the driver image is simply copied in the edit region of the input image (this provides a lower-bound on locality and faithfulness), (2) Inpainting: we use LDM [50] to inpaint the target edit region (this provide a lower-bound on naturalness), (3) Copy-Paste + DDIM Inversion + LDM Denoise: starting form copy-paste edit, we invert the image with DDIM, and denoise it with LDM, (4) E2EVE [5]. In Tab. 1 we report the quantitative results on the validation set

Model	FID (\downarrow)	L1 (\downarrow)	SSIM (\uparrow)
Copy-Paste (CP)	21.37	0.0	0.87
Inpainting [50]	8.25	0.02	0.17
CP + DDIM + LDM	9.15	0.02	0.32
E2EVE [5]	13.59	0.05	0.34
PAIR	12.81	0.02	0.51

Table 1: Results for In-Domain Localized Image Editing on the LSUN Bedroom validation set.



Figure 7: Visual results for in-domain localized image editing. We show the results obtained with relevant baselines for editing the red area in the input image using the reference as a driver.

of LSUN Bedroom [72]. We can notice that PAIR-Diffusion performs slightly better than E2EVE in terms of FID, and outperforms the previous method in terms of locality and faithfulness. Moreover, we observe that our method does not require specific training or data-collection procedures, but can solve editing tasks as a built-in property. We show a qualitative comparison with relevant baselines in Fig. 7, and refer the reader to *Supp. Mat.* for a detailed description of the evaluation procedure and baselines implementation.

Secondly, we evaluate the precision over structure control of our method. To assess it we compute the *mIoU* between the segmentation map used as conditioning (i.e. *S*), and the segmentation map obtained by applying another network to the final generated image. We obtained *mIoU* of 0.62, 0.43, 0.51 for the bedroom, church, and face datasets respectively. (see *Supp. Mat.* for additional details).

4.3. Discussion

In this work, we propose to edit images at the object level focusing on two important properties: appearance and structure. In general, these two represent independent as-

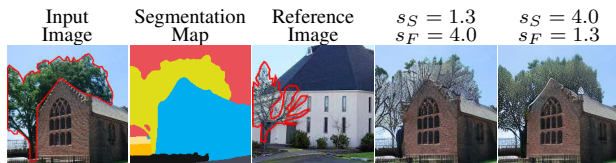


Figure 8: Effect of s_F and s_S in spatial classifier free guidance. Notice how the density of leaves increases with the structure spatial scale factor s_S .

pects of objects and our goal is to have full control over each of them. However, in some circumstances, the two can be highly dependent and the distinction is less obvious. For instance, consider the tree in Fig. 8. While the tree in the reference image is leafless, the one in the input has many leaves. In this situation, it is not obvious if the “density” of the leaves would be captured by the appearance or the structure information. In this case, spatial classifier-free guidance gives us a way to weigh the effect of appearance and structure on the final image at inference time. See *Supp. Mat.* for additional examples.

There can be many other design choices that allow us to obtain controllable object-level representations from a real image. We can introduce other control signals explicitly or factorize the appearance features into more elementary properties such as color and illumination. In future work, we plan to explore these directions and further improve the editing capabilities provided by the model.

5. Conclusion

In this paper, we introduce PAIR-Diffusion to tackle the task of object-level image editing. With our paired structure and appearance training of diffusion models, we obtain complex editing tasks enabling control over each component independently. We tested our method on several different scenarios: outdoor scenes, indoor scenes, and face images, showing remarkable editing capabilities in each of these. Our pipeline is efficient and is compatible with generative foundation models e.g. stable diffusion, further advancing the potential for creative applications.

References

- [1] Rameen Abdal, Yipeng Qin, and Peter Wonka. Image2stylegan: How to embed images into the stylegan latent space? In *Proceedings of the IEEE/CVF International Conference on Computer Vision*, pages 4432–4441, 2019. 3
- [2] Rameen Abdal, Yipeng Qin, and Peter Wonka. Image2stylegan++: How to edit the embedded images? In *Proceedings of the IEEE/CVF conference on computer vision and pattern recognition*, pages 8296–8305, 2020. 3
- [3] Omri Avrahami, Thomas Hayes, Oran Gafni, Sonal Gupta, Yaniv Taigman, Devi Parikh, Dani Lischinski, Ohad Fried, and Xi Yin. SpaText: Spatio-Textual Representation for Controllable Image Generation, Nov. 2022. arXiv:2211.14305 [cs]. 2, 15
- [4] Tim Brooks, Aleksander Holynski, and Alexei A Efros. Instructpix2pix: Learning to follow image editing instructions. *arXiv preprint arXiv:2211.09800*, 2022. 1, 2, 3
- [5] Andrew Brown, Cheng-Yang Fu, Omkar Parkhi, Tamara L. Berg, and Andrea Vedaldi. End-to-end visual editing with a generatively pre-trained artist. In *European Conference on Computer Vision (ECCV)*, 2022. 8, 13, 16
- [6] Holger Caesar, Jasper Uijlings, and Vittorio Ferrari. Coco-stuff: Thing and stuff classes in context. In *Proceedings of the IEEE conference on computer vision and pattern recognition*, pages 1209–1218, 2018. 15
- [7] Bowen Cheng, Ishan Misra, Alexander G. Schwing, Alexander Kirillov, and Rohit Girdhar. Masked-attention mask transformer for universal image segmentation. 2022. 12, 13
- [8] Shin-I Cheng, Yu-Jie Chen, Wei-Chen Chiu, Hung-Yu Tseng, and Hsin-Ying Lee. Adaptively-realistic image generation from stroke and sketch with diffusion model. In *Proceedings of the IEEE/CVF Winter Conference on Applications of Computer Vision*, pages 4054–4062, 2023. 3
- [9] Guillaume Couairon, Jakob Verbeek, Holger Schwenk, and Matthieu Cord. DiffEdit: Diffusion-based semantic image editing with mask guidance, Oct. 2022. arXiv:2210.11427 [cs]. 2
- [10] J. Deng, W. Dong, R. Socher, L.-J. Li, K. Li, and L. Fei-Fei. ImageNet: A Large-Scale Hierarchical Image Database. In *Proceedings of the IEEE/CVF Conference on Computer Vision and Pattern Recognition (CVPR)*, 2009. 12
- [11] Jiankang Deng, Jia Guo, Niannan Xue, and Stefanos Zafeiriou. Arcface: Additive angular margin loss for deep face recognition. In *Proceedings of the IEEE/CVF conference on computer vision and pattern recognition*, pages 4690–4699, 2019. 14
- [12] Prafulla Dhariwal and Alexander Nichol. Diffusion models beat gans on image synthesis. *Advances in Neural Information Processing Systems*, 34:8780–8794, 2021. 3
- [13] Dave Epstein, Taesung Park, Richard Zhang, Eli Shechtman, and Alexei A Efros. Blobgan: Spatially disentangled scene representations. In *Computer Vision—ECCV 2022: 17th European Conference, Tel Aviv, Israel, October 23–27, 2022, Proceedings, Part XV*, pages 616–635. Springer, 2022. 3
- [14] Wan-Cyuan Fan, Yen-Chun Chen, DongDong Chen, Yu Cheng, Lu Yuan, and Yu-Chiang Frank Wang. Frido: Feature Pyramid Diffusion for Complex Scene Image Synthesis, Aug. 2022. arXiv:2208.13753 [cs]. 3
- [15] Oran Gafni, Adam Polyak, Oran Ashual, Shelly Sheynin, Devi Parikh, and Yaniv Taigman. Make-a-scene: Scene-based text-to-image generation with human priors. In *Computer Vision—ECCV 2022: 17th European Conference, Tel Aviv, Israel, October 23–27, 2022, Proceedings, Part XV*, pages 89–106. Springer, 2022. 2, 3
- [16] Leon A Gatys, Alexander S Ecker, and Matthias Bethge. A neural algorithm of artistic style. *arXiv preprint arXiv:1508.06576*, 2015. 5, 12
- [17] Xinyu Gong, Shiyu Chang, Yifan Jiang, and Zhangyang Wang. Autogan: Neural architecture search for generative

- adversarial networks. In *Proceedings of the IEEE/CVF International Conference on Computer Vision*, pages 3224–3234, 2019. 3
- [18] Ian Goodfellow, Jean Pouget-Abadie, Mehdi Mirza, Bing Xu, David Warde-Farley, Sherjil Ozair, Aaron Courville, and Yoshua Bengio. Generative adversarial nets. In *Advances in Neural Information Processing Systems (NeurIPS)*, pages 2672–2680, 2014. 3
- [19] Ian Goodfellow, Jean Pouget-Abadie, Mehdi Mirza, Bing Xu, David Warde-Farley, Sherjil Ozair, Aaron Courville, and Yoshua Bengio. Generative adversarial networks. *Communications of the ACM*, 63(11):139–144, 2020. 3
- [20] Jiatao Gu, Alex Trevithick, Kai-En Lin, Josh Susskind, Christian Theobalt, Lingjie Liu, and Ravi Ramamoorthi. Nerfdiff: Single-image view synthesis with nerf-guided distillation from 3d-aware diffusion. *arXiv preprint arXiv:2302.10109*, 2023. 3
- [21] Amir Hertz, Ron Mokady, Jay Tenenbaum, Kfir Aberman, and Daniel Cohen-Or. Prompt-to-Prompt Image Editing with Cross Attention Control, Aug. 2022. *arXiv:2208.01626 [cs]*. 1, 2
- [22] Amir Hertz, Ron Mokady, Jay Tenenbaum, Kfir Aberman, Yael Pritch, and Daniel Cohen-Or. Prompt-to-prompt image editing with cross attention control. *arXiv preprint arXiv:2208.01626*, 2022. 3
- [23] Jonathan Ho, Ajay Jain, and Pieter Abbeel. Denoising diffusion probabilistic models. *Advances in Neural Information Processing Systems*, 33:6840–6851, 2020. 3, 5
- [24] Jonathan Ho and Tim Salimans. Classifier-Free Diffusion Guidance, July 2022. *arXiv:2207.12598 [cs]*. 5
- [25] Qingqing Huang, Daniel S Park, Tao Wang, Timo I Denk, Andy Ly, Nanxin Chen, Zhengdong Zhang, Zhishuai Zhang, Jiahui Yu, Christian Frank, et al. Noise2music: Text-conditioned music generation with diffusion models. *arXiv preprint arXiv:2302.03917*, 2023. 3
- [26] Dong Huk Park, Grace Luo, Clayton Toste, Samaneh Azadi, Xihui Liu, Maka Karalashvili, Anna Rohrbach, and Trevor Darrell. Shape-guided diffusion with inside-outside attention. *arXiv e-prints*, pages arXiv–2212, 2022. 2
- [27] Jitesh Jain, Jiachen Li, MangTik Chiu, Ali Hassani, Nikita Orlov, and Humphrey Shi. OneFormer: One Transformer to Rule Universal Image Segmentation. 2023. 2
- [28] Jitesh Jain, Anukriti Singh, Nikita Orlov, Zilong Huang, Jiachen Li, Steven Walton, and Humphrey Shi. Semask: Semantically masking transformer backbones for effective semantic segmentation. *arXiv*, 2021. 12, 13
- [29] Yifan Jiang, Shiyu Chang, and Zhangyang Wang. Transgan: Two transformers can make one strong gan. *arXiv preprint arXiv:2102.07074*, 2021. 3
- [30] Tero Karras, Timo Aila, Samuli Laine, and Jaakko Lehtinen. Progressive growing of gans for improved quality, stability, and variation. *arXiv preprint arXiv:1710.10196*, 2017. 3, 6
- [31] Tero Karras, Samuli Laine, and Timo Aila. A style-based generator architecture for generative adversarial networks. In *Proceedings of the IEEE/CVF conference on computer vision and pattern recognition*, pages 4401–4410, 2019. 3, 4
- [32] Gihyun Kwon and Jong Chul Ye. Diffusion-based image translation using disentangled style and content representation. *arXiv preprint arXiv:2209.15264*, 2022. 3
- [33] Mingi Kwon, Jaeseok Jeong, and Youngjung Uh. Diffusion Models already have a Semantic Latent Space, Oct. 2022. *arXiv:2210.10960 [cs]*. 2
- [34] Cheng-Han Lee, Ziwei Liu, Lingyun Wu, and Ping Luo. Maskgan: Towards diverse and interactive facial image manipulation. In *IEEE Conference on Computer Vision and Pattern Recognition (CVPR)*, 2020. 13
- [35] Xiang Lisa Li, John Thickstun, Ishaan Gulrajani, Percy Liang, and Tatsunori B Hashimoto. Diffusion-lm improves controllable text generation. *arXiv preprint arXiv:2205.14217*, 2022. 3
- [36] Jun Hao Liew, Hanshu Yan, Daquan Zhou, and Jiashi Feng. MagicMix: Semantic Mixing with Diffusion Models, Oct. 2022. *arXiv:2210.16056 [cs]*. 1, 2
- [37] Gautam Mittal, Jesse Engel, Curtis Hawthorne, and Ian Simon. Symbolic music generation with diffusion models. *arXiv preprint arXiv:2103.16091*, 2021. 3
- [38] Ron Mokady, Amir Hertz, Kfir Aberman, Yael Pritch, and Daniel Cohen-Or. Null-text inversion for editing real images using guided diffusion models. *arXiv preprint arXiv:2211.09794*, 2022. 3
- [39] Alex Nichol, Prafulla Dhariwal, Aditya Ramesh, Pranav Shyam, Pamela Mishkin, Bob McGrew, Ilya Sutskever, and Mark Chen. Glide: Towards photorealistic image generation and editing with text-guided diffusion models. *arXiv preprint arXiv:2112.10741*, 2021. 3
- [40] Taesung Park, Ming-Yu Liu, Ting-Chun Wang, and Jun-Yan Zhu. Semantic image synthesis with spatially-adaptive normalization. In *Proceedings of the IEEE/CVF conference on computer vision and pattern recognition*, pages 2337–2346, 2019. 3
- [41] Gaurav Parmar, Krishna Kumar Singh, Richard Zhang, Yijun Li, Jingwan Lu, and Jun-Yan Zhu. Zero-shot image-to-image translation. *arXiv preprint arXiv:2302.03027*, 2023. 3
- [42] Or Patashnik, Zongze Wu, Eli Shechtman, Daniel Cohen-Or, and Dani Lischinski. Styleclip: Text-driven manipulation of stylegan imagery. In *Proceedings of the IEEE/CVF International Conference on Computer Vision*, pages 2085–2094, 2021. 3
- [43] Guim Perarnau, Joost Van De Weijer, Bogdan Raducanu, and Jose M Álvarez. Invertible conditional gans for image editing. *arXiv preprint arXiv:1611.06355*, 2016. 3
- [44] Ben Poole, Ajay Jain, Jonathan T Barron, and Ben Mildenhall. Dreamfusion: Text-to-3d using 2d diffusion. *arXiv preprint arXiv:2209.14988*, 2022. 3
- [45] Lu Qi, Jason Kuen, Yi Wang, Jiuxiang Gu, Hengshuang Zhao, Philip Torr, Zhe Lin, and Jiaya Jia. Open world entity segmentation. *IEEE Transactions on Pattern Analysis and Machine Intelligence*, 2022. 2
- [46] Alec Radford, Jong Wook Kim, Chris Hallacy, Aditya Ramesh, Gabriel Goh, Sandhini Agarwal, Girish Sastry, Amanda Askell, Pamela Mishkin, Jack Clark, et al. Learning transferable visual models from natural language supervision. In *International conference on machine learning*, pages 8748–8763. PMLR, 2021. 3

- [47] Alec Radford, Luke Metz, and Soumith Chintala. Unsupervised representation learning with deep convolutional generative adversarial networks. *arXiv preprint arXiv:1511.06434*, 2015. 3
- [48] Aditya Ramesh, Prafulla Dhariwal, Alex Nichol, Casey Chu, and Mark Chen. Hierarchical text-conditional image generation with clip latents. *arXiv preprint arXiv:2204.06125*, 2022. 3
- [49] Aditya Ramesh, Prafulla Dhariwal, Alex Nichol, Casey Chu, and Mark Chen. Hierarchical Text-Conditional Image Generation with CLIP Latents, Apr. 2022. arXiv:2204.06125 [cs]. 3
- [50] Robin Rombach, Andreas Blattmann, Dominik Lorenz, Patrick Esser, and Björn Ommer. High-resolution image synthesis with latent diffusion models. In *Proceedings of the IEEE/CVF Conference on Computer Vision and Pattern Recognition*, pages 10684–10695, 2022. 2, 3, 4, 5, 8, 12, 13, 15
- [51] Mozhddeh Rouhsedaghat, Masoud Monajatipoor, Kai-Wei Chang, C-C Jay Kuo, and Iacopo Masi. Magic: Mask-guided image synthesis by inverting a quasi-robust classifier. *arXiv preprint arXiv:2209.11549*, 2022. 3
- [52] Nataniel Ruiz, Yuanzhen Li, Varun Jampani, Yael Pritch, Michael Rubinstein, and Kfir Aberman. DreamBooth: Fine Tuning Text-to-Image Diffusion Models for Subject-Driven Generation, Aug. 2022. arXiv:2208.12242 [cs]. 2
- [53] Chitwan Saharia, William Chan, Saurabh Saxena, Lala Li, Jay Whang, Emily Denton, Seyed Kamyar Seyed Ghasemipour, Burcu Karagol Ayan, S Sara Mahdavi, Rapha Gontijo Lopes, et al. Photorealistic text-to-image diffusion models with deep language understanding. *arXiv preprint arXiv:2205.11487*, 2022. 3
- [54] Tim Salimans and Jonathan Ho. Progressive distillation for fast sampling of diffusion models. *arXiv preprint arXiv:2202.00512*, 2022. 3
- [55] Christoph Schuhmann, Richard Vencu, Romain Beaumont, Robert Kaczmarczyk, Clayton Mullis, Aarush Katta, Theo Coombes, Jenia Jitsev, and Aran Komatsuzaki. Laion-400m: Open dataset of clip-filtered 400 million image-text pairs, 2021. 15
- [56] Karen Simonyan and Andrew Zisserman. Very deep convolutional networks for large-scale image recognition. In *International Conference on Learning Representations (ICLR)*, 2015. 12
- [57] Uriel Singer, Shelly Sheynin, Adam Polyak, Oron Ashual, Iurii Makarov, Filippos Kokkinos, Naman Goyal, Andrea Vedaldi, Devi Parikh, Justin Johnson, et al. Text-to-4d dynamic scene generation. *arXiv preprint arXiv:2301.11280*, 2023. 3
- [58] Jascha Sohl-Dickstein, Eric Weiss, Niru Maheswaranathan, and Surya Ganguli. Deep unsupervised learning using nonequilibrium thermodynamics. In *International Conference on Machine Learning*, pages 2256–2265. PMLR, 2015. 3
- [59] Jiaming Song, Chenlin Meng, and Stefano Ermon. Denoising diffusion implicit models. *arXiv preprint arXiv:2010.02502*, 2020. 4, 5
- [60] Yang Song and Stefano Ermon. Generative modeling by estimating gradients of the data distribution. *Advances in neural information processing systems*, 32, 2019. 12, 13
- [61] Narek Tumanyan, Michal Geyer, Shai Bagon, and Tali Dekel. Plug-and-Play Diffusion Features for Text-Driven Image-to-Image Translation, Nov. 2022. arXiv:2211.12572 [cs]. 1, 2
- [62] Arash Vahdat, Karsten Kreis, and Jan Kautz. Score-based generative modeling in latent space. *Advances in Neural Information Processing Systems*, 34:11287–11302, 2021. 3
- [63] Andrey Voynov, Kfir Aberman, and Daniel Cohen-Or. Sketch-Guided Text-to-Image Diffusion Models, Nov. 2022. arXiv:2211.13752 [cs]. 1, 2
- [64] Weilun Wang, Jianmin Bao, Wengang Zhou, Dongdong Chen, Dong Chen, Lu Yuan, and Houqiang Li. Semantic image synthesis via diffusion models. *arXiv preprint arXiv:2207.00050*, 2022. 3
- [65] Christopher KI Williams. Structured generative models for scene understanding. *arXiv preprint arXiv:2302.03531*, 2023. 4
- [66] Qiucheng Wu, Yujian Liu, Handong Zhao, Ajinkya Kale, Trung Bui, Tong Yu, Zhe Lin, Yang Zhang, and Shiyu Chang. Uncovering the disentanglement capability in text-to-image diffusion models. *arXiv preprint arXiv:2212.08698*, 2022. 2
- [67] Wenqi Xian, Patsorn Sangkloy, Varun Agrawal, Amit Raj, Jingwan Lu, Chen Fang, Fisher Yu, and James Hays. Texturegan: Controlling deep image synthesis with texture patches. In *Proceedings of the IEEE conference on computer vision and pattern recognition*, pages 8456–8465, 2018. 3
- [68] DeJia Xu, Yifan Jiang, Peihao Wang, Zhiwen Fan, Yi Wang, and Zhangyang Wang. Neurrallift-360: Lifting an in-the-wild 2d photo to a 3d object with 360° views. *arXiv e-prints*, pages arXiv–2211, 2022. 3
- [69] Xingqian Xu, Zhangyang Wang, Eric Zhang, Kai Wang, and Humphrey Shi. Versatile diffusion: Text, images and variations all in one diffusion model, 2022. 3
- [70] Zhengyuan Yang, Jianfeng Wang, Zhe Gan, Linjie Li, Kevin Lin, Chenfei Wu, Nan Duan, Zicheng Liu, Ce Liu, Michael Zeng, and Lijuan Wang. ReCo: Region-Controlled Text-to-Image Generation, Nov. 2022. arXiv:2211.15518 [cs]. 2, 3
- [71] Jason Yosinski, Jeff Clune, Anh Nguyen, Thomas Fuchs, and Hod Lipson. Understanding neural networks through deep visualization. *arXiv preprint arXiv:1506.06579*, 2015. 5, 12
- [72] Fisher Yu, Ari Seff, Yinda Zhang, Shuran Song, Thomas Funkhouser, and Jianxiong Xiao. Lsun: Construction of a large-scale image dataset using deep learning with humans in the loop. *arXiv preprint arXiv:1506.03365*, 2015. 6, 8, 12, 13, 15
- [73] Matthew D Zeiler and Rob Fergus. Visualizing and understanding convolutional networks. In *Computer Vision—ECCV 2014: 13th European Conference, Zurich, Switzerland, September 6–12, 2014, Proceedings, Part I 13*, pages 818–833. Springer, 2014. 5
- [74] Yu Zeng, Zhe Lin, Jianming Zhang, Qing Liu, John Colomosse, Jason Kuen, and Vishal M. Patel. SceneCom-

poser: Any-Level Semantic Image Synthesis, Nov. 2022. arXiv:2211.11742 [cs]. 2

- [75] Yu Zeng, Zhe Lin, Jianming Zhang, Qing Liu, John Colomosse, Jason Kuen, and Vishal M Patel. Scenecomposer: Any-level semantic image synthesis. *arXiv preprint arXiv:2211.11742*, 2022. 3
- [76] Lvmin Zhang and Maneesh Agrawala. Adding conditional control to text-to-image diffusion models. *arXiv preprint arXiv:2302.05543*, 2023. 2, 3, 15
- [77] Bolei Zhou, Hang Zhao, Xavier Puig, Sanja Fidler, Adela Barriuso, and Antonio Torralba. Scene parsing through ade20k dataset. In *Proceedings of the IEEE conference on computer vision and pattern recognition*, pages 633–641, 2017. 12, 13
- [78] Jun-Yan Zhu, Philipp Krähenbühl, Eli Shechtman, and Alexei A Efros. Generative visual manipulation on the natural image manifold. In *Computer Vision—ECCV 2016: 14th European Conference, Amsterdam, The Netherlands, October 11–14, 2016, Proceedings, Part V 14*, pages 597–613. Springer, 2016. 3
- [79] Peihao Zhu, Rameen Abdal, Yipeng Qin, and Peter Wonka. Sean: Image synthesis with semantic region-adaptive normalization. In *Proceedings of the IEEE/CVF Conference on Computer Vision and Pattern Recognition*, pages 5104–5113, 2020. 2, 3, 13

A. Implementation Details

In this section, we provide additional details for training and inferencing the model. To extract the structure information, we apply SeMask-L [28] with Mask2former [7] trained on ADE20K [77], and compute the segmentation mask for LSUN Church and Bedroom datasets [72]. In CelebA-HQ, ground truth segmentation masks are available. To compute the appearance vectors, we use VGG [56] pre-trained on ImageNet-1K [10] as the appearance model $E_F(\cdot)$ in Eq. (3). Specifically, we take the features after the ninth layer of the network to retain more low-level information [16, 71]. The resulting appearance features $F \in \mathbb{R}^{N \times C}$ are splatted using the segmentation map $S \in \mathbb{N}^{H \times W}$, resulting in a tensor of shape $F' \in \mathbb{R}^{C \times H \times W}$. Then the LDM [50] is conditioned by concatenating S , F' , and the noisy latent z_t along the channels dimension. Note that, we $L2$ normalize the appearance features F' before the concatenation. We increase the number of channels of the first convolutional layer of the U-Net from C_{in} to $C_{in} + C + 1$ and keep the rest of the architecture as in [50]. For all three datasets namely, LSUN Church, Bedroom, and CelebA-HQ we start with the pre-trained weights provided by LDM [50] and finetune with exactly the same hyperparameters mentioned in the paper [50]. The number of steps, learning rate, and batch size are reported in Tab 2. We train our models using A100 GPUs.

At inference time, we apply the DDIM algorithm [60] with 250 steps. In general, for *In Domain Appearance Manipulation*, we used $s_F = 1.3$ and $s_S = 1.3$, whereas for

Dataset	lr	batch size	Iterations
Bedroom	9.6e-5	48	750k
Churches	1.0e-5	96	350k
CelebA-HQ	9.6e-5	24	120k

Table 2: Hyperparameters for PAIR diffusion

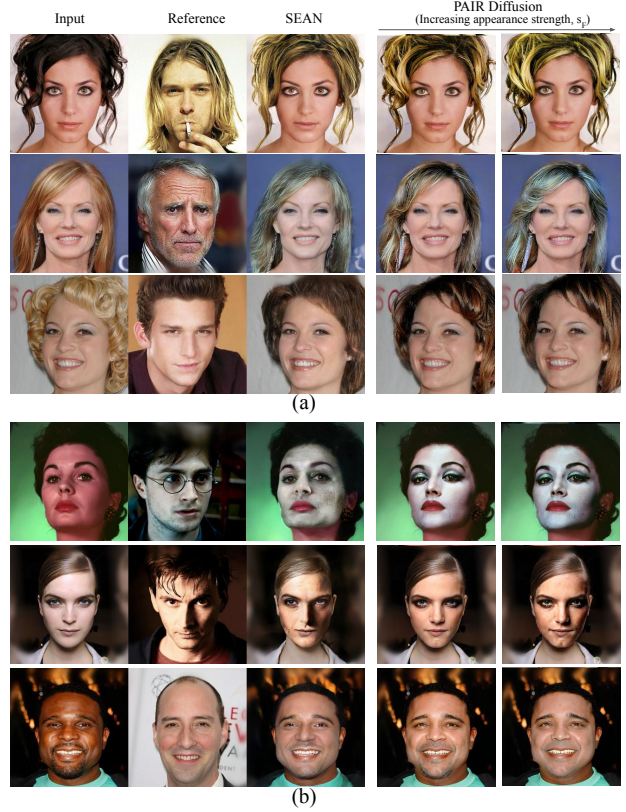


Figure 9: We edit hairs (a) and skin (b) in the input image from the reference image. PAIR diffusion allows controlling the strength of appearance injection which is not provided by other methods.

Out of Domain Appearance Manipulation we used $s_F = 3.0$ and $s_S = 1.3$ through out the spatial location. To perform local edits, we rely on the masked DDIM technique presented in the inpainting model of [50]. In detail, let $\mathcal{R} \in \{0, 1\}^{H \times W}$ denote the area of the input image x where we want to perform the edit. We apply DDIM inversion to the input image x , and obtain \hat{z}_t . Next, during the denoising process we combine the output of the diffusion model with the inverted image as:

$$z_{t-1} = \mathcal{R} \cdot \epsilon_\theta(z_t, S, F) + (1 - \mathcal{R}) \cdot \hat{z}_{t-1} \quad (7)$$

and iterate for $t \in [T, \dots, 1]$.

B. Baseline Comparison

In this section, we provide additional details about implementation and evaluation procedures for the results shown in Sec. 4.2 of the main paper. We evaluate the models on the task of in-domain appearance manipulation. We first describe the data-collection procedure. We use 5000 images from the validation set of LSUN Bedroom, and choose the bed as the object to edit. For each image, we randomly select a patch within the bed, and use a patch extracted in the same way from another image as the driver for the edit. Next, we describe the baselines. **Copy-Paste**: the target patch is copied and pasted in the target region of the input image, resizing the patch to fit the target region. **Inpainting**, we use the model pretrained on LSUN Bedroom Dataset by [50], and use it to inpaint the edit region. To do that, we use masked-DDIM sampling, as described in Eq.(7). **CP+DDIM+LDM**, we start from the results of copy-paste and apply DDIM Inversion to map the image to the diffusion noise space [60]. Subsequently, we apply LDM to denoise the image to the final result. Lastly, we compare our method with **E2EVE** [5]. We use the original pre-trained weights shared by the authors, and use their model to perform the edit. Next, we detail the metrics calculation pipeline. We compute *naturalness* by measuring the FID between the edited images and the original images from the whole dataset. We estimate the *locality*, by measuring the L1 loss between the original image and the edited image outside the edited region (i.e. the region that should not change). Finally, the *faithfulness* is measured by the SSIM between the driver image and the edited region in the edited image. We provide an additional qualitative comparison between the baselines and our method in Fig.12.

In order to compute the mIoU reported in Sec. 4.2, we first generate the images using appearance and structure information from the images in the validation dataset and then segment them. For LSUN churches and bedroom [72] we used SeMask-L [28] with Mask2former [7] trained on ADE20K [77], while for CelebA-HQ [34] we used the official public available code. In the case of the church and bedroom dataset, we used major classes for calculating the mIoU because the performance of the segmentation model drops significantly for less frequent classes. Namely, we use *building, sky, tree, road, grass, person* classes for LSUN churches and *wall, floor, ceiling, bed, window, lamp* classes for LSUN bedrooms. In case of CelebA-HQ we used all the classes. Following the above procedure we got the reported mIoU of 0.62, 0.43, 0.51 for the bedroom, church, and face datasets respectively.

A closely related work to PAIR diffusion in GANs is SEAN [79]. However, SEAN [79] does not provide a mechanism to independently weigh the importance of structure

and appearance while editing which can be done using the proposed spatial classifier free guidance in our method. Please refer to Fig. 9 for visual results. We used $s_S = 1.3, s_F = 1.3$ and $s_S = 1.3, s_F = 3$ to get the results. We can see that we can control the intensity of the color in rows 1 and 2, Fig. 9(a). Further, we can also increase the intensity of the texture of the reference image as can be seen in row 3 (Fig. 9(a)) where the hairs become straighter as we increase s_F . Similar observations can be made when we edit the skin in Fig. 9(b). We can increase the color intensity and shadow effect in rows 1 and 2 respectively. Further, we are also able to control the strength of the beard in row 3. When we increase the strength of the reference appearance, the beard disappears as there is no beard in the reference image. Overall the visual quality of the editing looks more natural for PAIR diffusion. Note, when using SEAN we used the official pre-trained weights of [79] to make the edits.

C. Qualitative Results

We provide additional qualitative results for the task of In Domain Appearance Manipulation in Fig. 13. We can observe that our method seamlessly transfers the appearance from the reference image to the input image. Instead of simply swapping the appearance of input and reference images (i.e. setting $\alpha = 0, \beta = 1$ in Eq.(5)), we can obtain more nuanced results by linearly combining the two. In Fig. 14, we exploit this direction defining $\beta = \lambda, \alpha = 1 - \lambda$ and varying λ from 0 to 1, i.e. interpolating input and reference images. We can notice how the appearance of the edited region smoothly transitions from the original appearance to the reference, providing an additional level of control for the end user. Lastly, we present more results for the task of Out of Domain Appearance Manipulation, both in the setting of global editing in Fig. 15 and local editing in Fig. 16.

D. Discussion

In this section, we discuss the role of *structure* and *appearance* and the level of control we can achieve with PAIR-Diffusion. As described in Sec. 3.1 of the main paper, we represent the i -th object as $o_i = \{s_i, f_i, \pi_i\}$ and assume an image is composed by N of such objects. In this formulation, s_i contains the structure information, and f_i represents the appearance information. π_i represents all other information associated with the i -th object which we decide to do not explicitly control; these are modeled by the noise.

First, we discuss the interaction between structure s_i and the appearance f_i . According to the definition given in Eq. (3), the appearance features f_i depend on the respective shape m_i of the object. In particular, we observe that if the segmentation map is coarse (e.g. covering the whole facade of a church without distinguishing windows

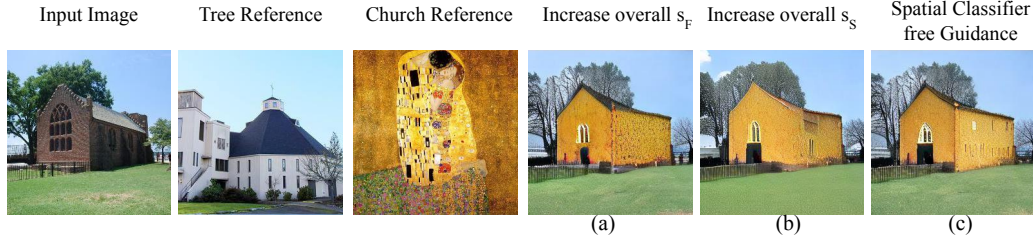


Figure 11: With spatial classifier-free guidance we can control the appearance of the tree and church independently and get desired results.

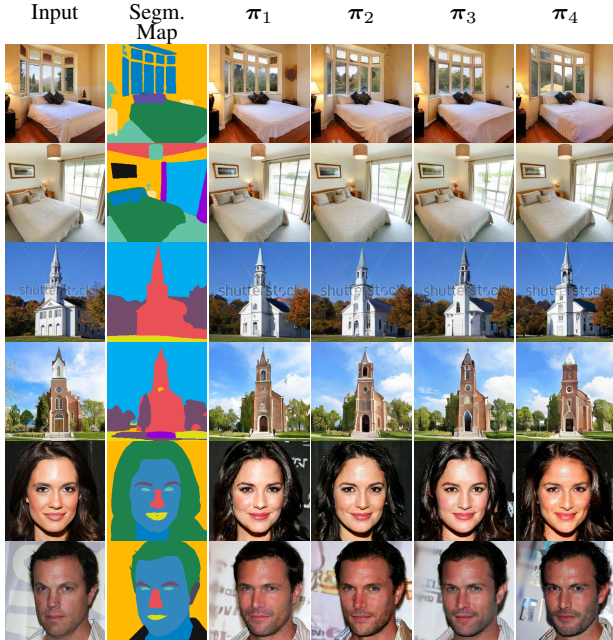


Figure 10: Variations in the image by keeping structure and appearance fixed for all the objects, and sampling using different noises $\pi_k \sim \mathcal{N}(0, 1)$.

or doors), the correspondent appearance vector will contain some information about the structure (*i.e.* the presence of windows or doors). Whereas, if the segmentation map is fine-grained (*e.g.* bed and pillow are represented using separate segments) the appearance vector would mostly contain the low-level details such as color, texture, and illumination.

To have a better understanding of the above discussion and the information contained in π_i , we generate images by sampling $\pi \sim \mathcal{N}(0, 1)$ (with $\pi = \{\pi_i\}_{i \in [1, \dots, N]}$ as defined in Sec. 3) and keeping s_i and f_i fixed for all the objects in the image. The results are shown in Fig. 10. We can observe that in the case of bedrooms (first and second row), there are only subtle changes in the appearance of the objects. This is in line with the previous discussion because, in the case of bedrooms, the segmentation maps are fine-grained hence the appearance of the objects is completely defined. We can

see some variations in reflections, and scenes outside the window because it is not controlled by structure or appearance and is majorly controlled by the noise. Vice-versa, in the case of churches (third and fourth rows), we observe that by sampling different noises, we get variations in terms of position and details of doors and windows in the building. Analyzing the associated segmentation map, we can observe that they are coarse and don't provide fine-grained details, *e.g.* about the position of the windows and doors of the building. Hence, this information will be controlled by π . Nevertheless, even with for different noises, the overall appearance remains faithful to the input image. In the case of faces (last two rows), we have a fine-grained segmentation map and the variations are mostly in accordance with the input image. We can see some changes in the color of skin and lips but we believe it is because VGG features are not sensitive enough for subtle changes in the face color. We expect to get even more fine-grained control over color in the case of faces if we use features from a face identification network [11].

Lastly, we show the utility of the proposed spatial classifier guidance. Spatial classifier-free guidance helps us to improve the independent control of the appearance and structure of individual objects. This can be highly useful when editing multiple objects at once and they have different requirements for structure and appearance guidance. We show such a use case in Fig. 11. Given an input image, we use two reference images to target two objects of the input: the tree and the church. Assume we would like to give more preference to the appearance of the tree from the reference image. We can see that if we simply increase s_F for all the objects, the church starts relying too much on its reference image and starts losing details (Fig. 11(a)). Conversely, if we increase s_S for the whole image the church starts looking better but the tree becomes dense, which is different from its reference image, Fig. 11(b). We can achieve the desired edit only by using spatial classifier-free guidance, increasing the value of s_F for the tree and s_S for the church independently, and get the image in Fig. 11(c).

E. PAIR Diffusion for Foundation Models

We further extend our method to foundation generative models, in particular Stable Diffusion [50]. Stable Diffusion [50] is a text-to-image model trained on a large corpus of data [55], thus can be leveraged to edit images in the wild. Differently from images in the LSUN Church or Bedroom datasets [72], images in the wild can be more complex and have multiple objects with the same category. Nevertheless, each object will have its own appearance and we seek independent control over all of them. For these reasons, we use panoptic segmentation masks to get the per-object-mask m_i which is used in Eq. (3) to get the appearance feature f_i . To summarize, in text-to-image models we need to learn $p(x|S, F, T)$ to achieve our aim, where we use the semantic segmentation mask to represent the structure information S , but adopt the panoptic segmentation mask to pool per-object appearance features F . Lastly, we condition the model on text prompt T , which is provided through the original cross-attention mechanism. Similarly to Spa-Text [3], fine-tuning Stable Diffusion directly in our setting would require millions of images with the corresponding segmentation maps, appearance features, and text caption; however, such a dataset is difficult to collect and involves huge computation. Recently, Zhang *et. al.* proposed ControlNet [76] to efficiently add controlling signals to Stable Diffusion using fewer data points and training iterations. As discussed in Sec. 3.1, we seek a mechanism to condition the generative model and realize $p(x|S, F, T)$. Due to its efficiency, we rely on ControlNet [76] to enable structure and appearance control in Stable Diffusion. In order to incorporate text conditioning we also extend the spatial classifier-free guidance as shown below

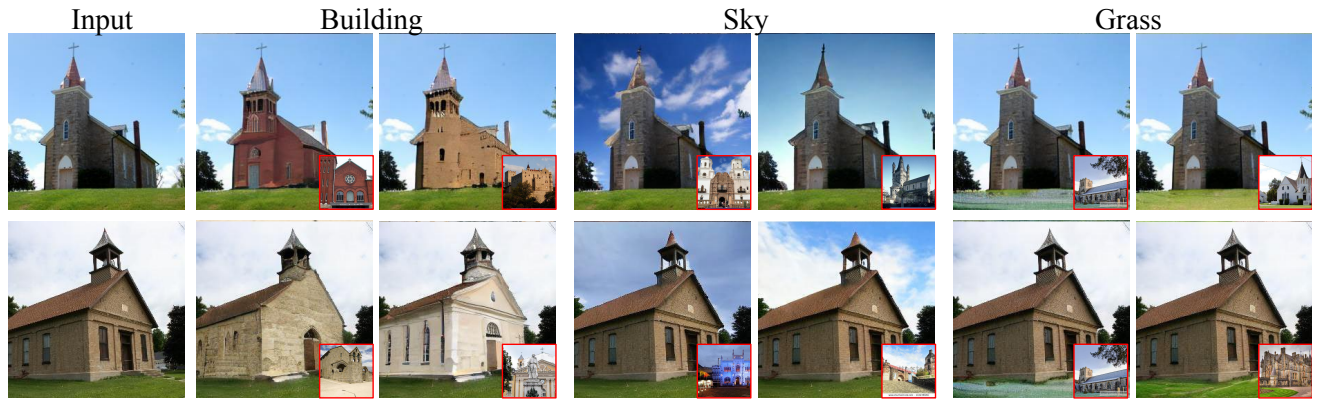
$$\begin{aligned} \tilde{\epsilon}_\theta(z_t, S, F, T) = & \epsilon_\theta(z_t, \emptyset, \emptyset, \emptyset) \\ & + s_S \cdot (\epsilon_\theta(z_t, S, \emptyset, \emptyset) - \epsilon_\theta(z_t, \emptyset, \emptyset, \emptyset)) \\ & + s_F \cdot (\epsilon_\theta(z_t, S, F, \emptyset) - \epsilon_\theta(z_t, S, \emptyset, \emptyset)) \\ & + s_T \cdot (\epsilon_\theta(z_t, S, F, T) - \epsilon_\theta(z_t, S, F, \emptyset)) \end{aligned} \tag{8}$$

where factors $s_S, s_F, s_T \in \mathbb{R}^{H \times W}$, and $\epsilon_\theta(z_t, S, F, T)$ represents the learned diffusion model.

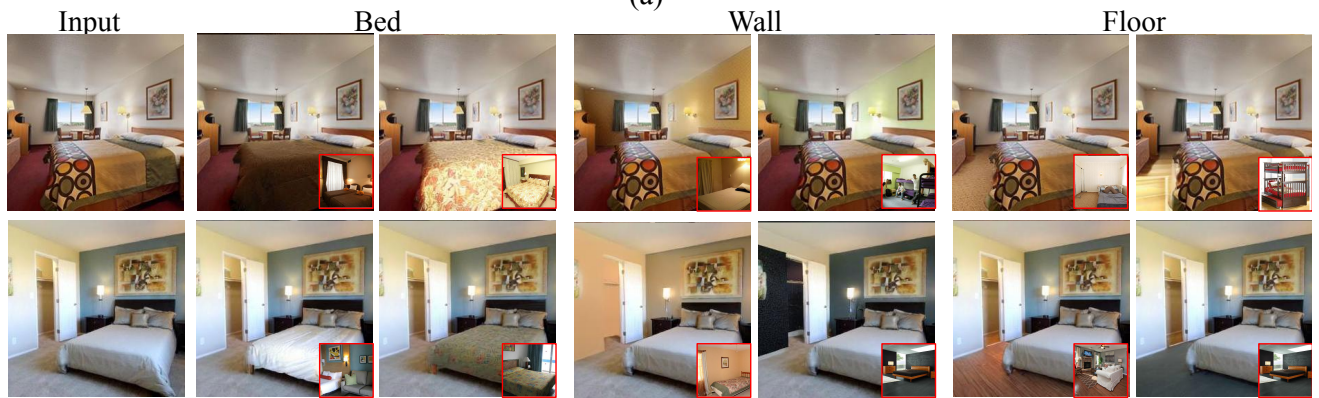
We use COCO Stuff [6] dataset for training, which contains annotations for semantic and panoptic segmentation along with image captions. We used the training split of roughly 118K images to train the model and fine-tune the model for 60,000 iterations. We use the validation split of 5000 images to save the best model.



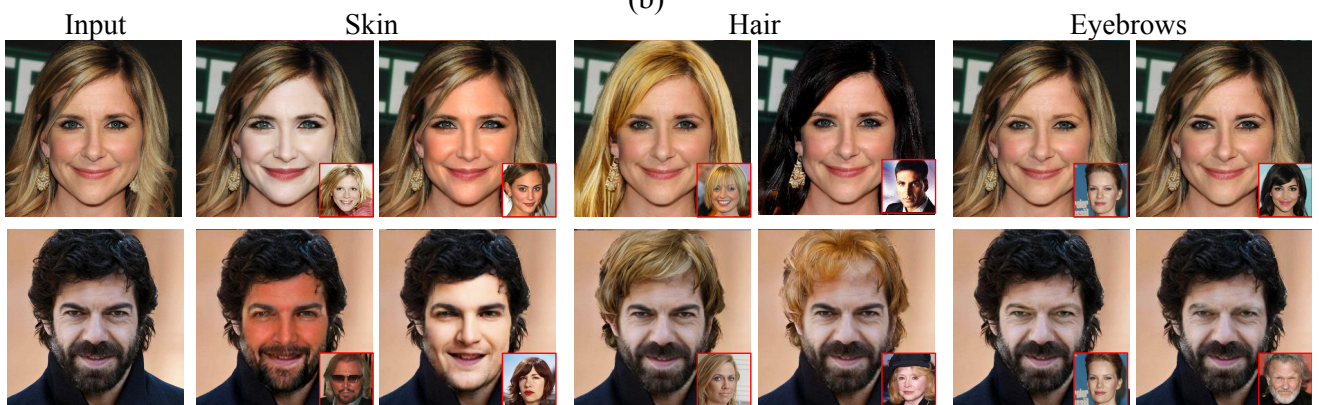
Figure 12: Visual results for in-domain localized image editing. We edit the input image, using as driver the reference image, targeting the red-boxed area. With PAIR-Diffusion we can perform realistic edits in challenging scenarios. For example, in the first row, we can use the entire bed as a driver and edit only a patch of the input image. On the contrary, in the last row, we use a small patch as driver and target the whole bed of the input image for the edit. In both cases, our method outputs realistic edited images. Moreover, due to the masked DDIM technique we introduce almost no distortion in the area outside the red box (*i.e.* the one that should not change). We show results for all the baselines.



(a)



(b)



(c)

Figure 13: Qualitative results for in-domain appearance manipulation

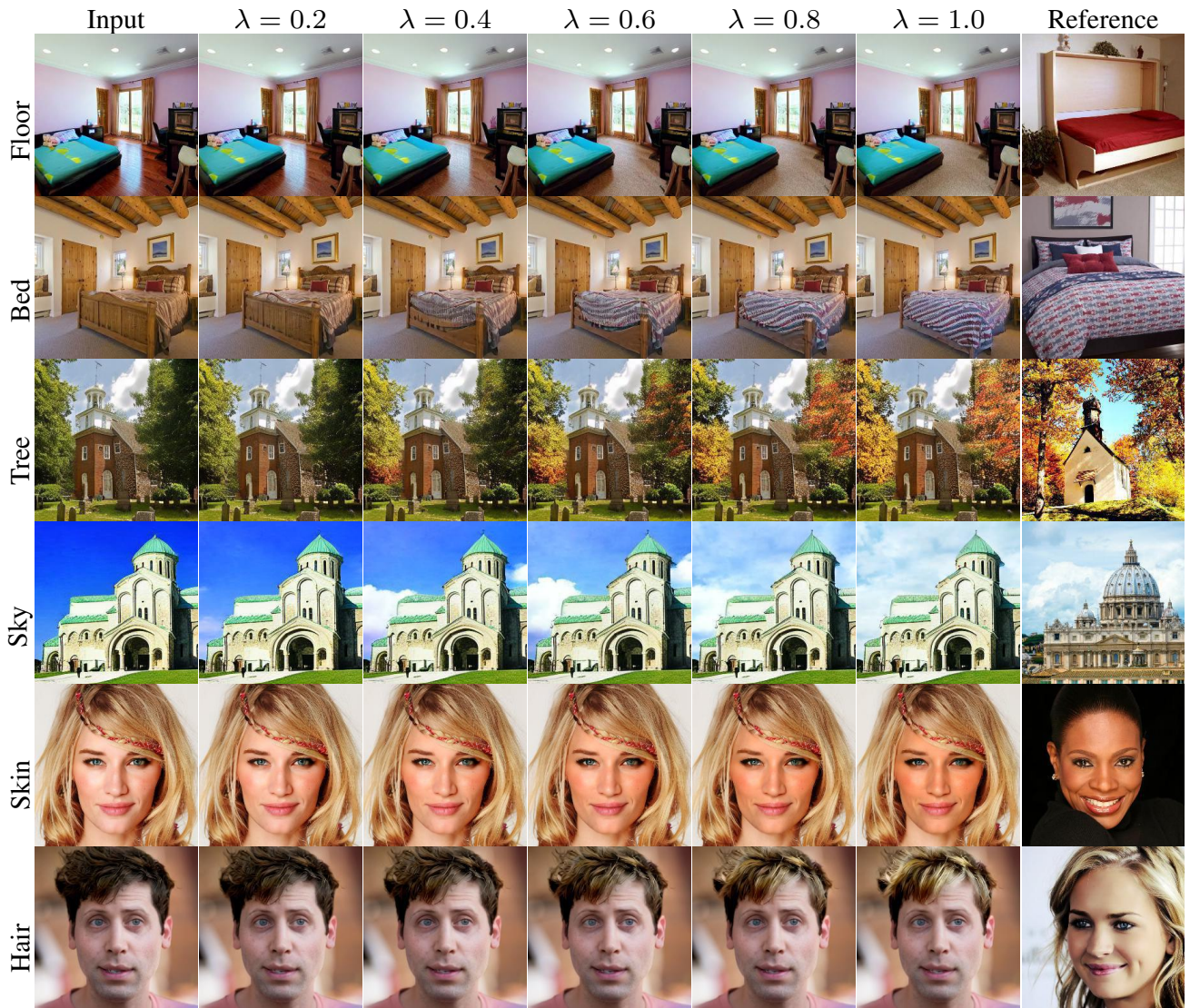


Figure 14: We can control the strength of appearance and interpolate between the reference and input appearances. We set $\alpha = 1 - \lambda$ and $\beta = \lambda$ in Eq. (5) and vary λ from 0 to 1.



Figure 15: Visual results for out of domain global appearance manipulation.

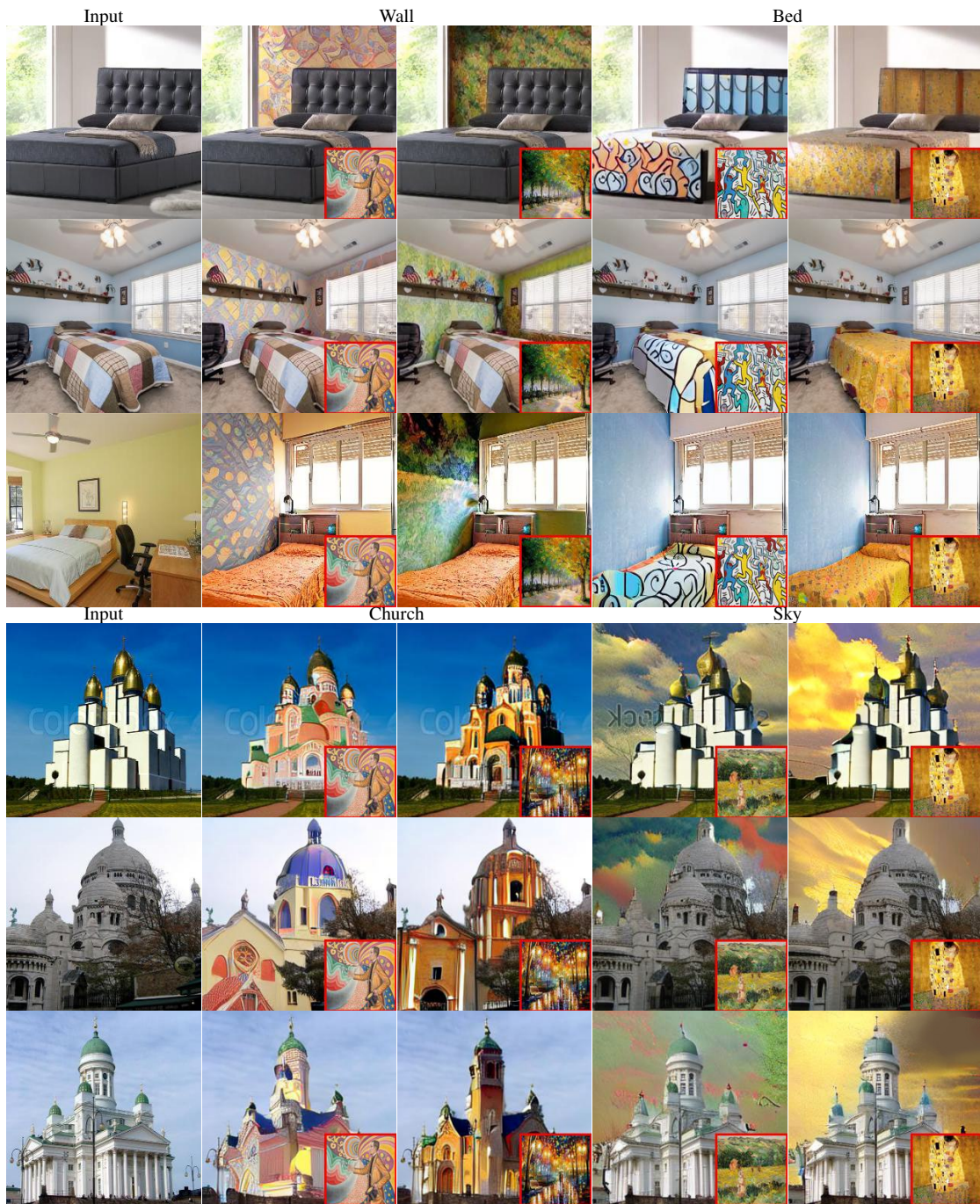


Figure 16: Visual results for out of domain local appearance manipulation.